Tech Science Press

Research on Key Technologies of Electronic Shelf Labels Based on LoRa

Malak Abid Ali Khan[1,2], Xiaofeng Lian[1,*], Imran Khan Mirani[1,3] and Li Tan[4]

[1]School of Artificial Intelligence, Beijing Technology & Business University, Beijing, 100048, China
[2]School of Automation, Beijing Institute of Technology, Beijing, 100081, China
[3]School of Information and Computer Engineering, Beijing University of Technology, Beijing, 100124, China
[4]School of Computer Science & Engineering, Beijing Technology & Business University, Beijing, 100048, China
[*]Corresponding Author: Xiaofeng Lian. Email: lianxf@th.btbu.edu.cn

Abstract: The demand for Electronic Shelf Labels (ESL), according to the Internet of Things (IoT) paradigm, is expected to grow considerably in the immediate future. Various wireless communication standards are currently contending to gain an edge over the competition and provide the massive connectivity that will be required by a world in which everyday objects are expected to communicate with each other. Low-Power Wide-Area Networks (LPWANs) are continuously gaining momentum among these standards, mainly thanks to their ability to provide long-range coverage to devices, exploiting license-free frequency bands. The main theme of this work is one of the most prominent LPWAN technologies, LoRa. The purpose of this research is to provide long-range, less intermediate node, less energy dissipation, and a cheaper ESL system. Much research has already been done on designing the LoRaWAN network, not capable to make a reliable network. LoRa is using different gateways to transmit the same data, collision, data jamming, and data repetition are expected. According to the transmission behavior of LoRa, 50% of data is lost. In this paper, the Improved Backoff Algorithm with synchronization technique is used to decrease overlapping and data loss. Besides, the improved Adaptive Data Rate algorithm (ADR) avoids the collision in concurrently transmitted data by using different Spreading Factors (SFs). The allocation of SF has the main role in designing LoRa based network to minimize the impact of the intra-interference, cost function, and Euclidean distance. For this purpose, the K-means machine learning algorithm is used for clustering. The data rate model is using an intra-slicing technique based on Maximum Likelihood Estimation (MLE). The data rate model includes three critical communication slices, High Critical Communication (HCC), Medium Critical Communication (MCC), and Low Critical Communication (LCC), having the specified number of End devices (EDs), payload budget delay, and data rate. Finally, different combinations of gateways are used to build ESL for 200 electronic shelf labels.

Keywords: LoRa; electronic shelf labels; adaptive data rate; backoff algorithm; remote Acknowledgment

1 Introduction

In recent years, many companies are using Electronic Shelf Label System (ESLS) that usually work on infrared or radio frequency network, and has been brought into some retailers for getting real-time wireless updating and displaying of shelf labels information [1]. To operate properly for ESL, the wireless communication network needs to have a reasonable range, data rate, battery life, robustness, and

reliability. A variety of wireless communications, such as Near Field Communication (NFC), Radio Frequency Identification (RFID), Bluetooth, and Wi-Fi, can be used but each of these has drawbacks and limitations. For example, NFC and RFID have the problem of short recognition distance, and Bluetooth and Wi-Fi have difficulties in individualized identification due to a wide antenna beam pattern, and illuminating technology had other limitations. Moreover, the cost increases in ESL tag manufacturing are another major issue [2–3]. The previous ESL system has a high data rate but a limited range and high cost. The latest technologies used for ESL are based on, QR codes, BLE (Bluetooth low-Energy), and NFC [4]. These are one of the fast and easy install technologies in the market right now but it has some limitations which make it unusable for big shopping malls, supermarkets, and warehouses. These technologies have a limited communication range and high energy consumptions as compared to other wireless standards. LoRa is a long-range technology that can transmit data up to 15 kilometers with minimum energy consumptions. Tab. 1 gives information about DR, power consumption, range, and battery drainage of the LPWN technologies [5–7].

Table 1: Comparison of different wireless standards

Wireless standards	Power consumption	Transmission range	Data rates
Bluetooth	Medium	1~100 m	1~3 Mbps
Bluetooth LE	Lower	>100 m	125 kbps~2 Mbps
LoRaWAN	Low	10 km	0.3~50 kbps
NB-IoT	Low	<35 km	20 kbps~5 Mbps
NFC	Low	<10 cm	106~424 kbps
Sigfox	Low	3~50 km	100~600 kbps
6LoWPAN	Low	100 m	0~250 kbps
Wi-Fi	Medium	100 m	10~100 + Mbps
Zigbee	Low	10~100 m	20~250 kbps
Z-wave	Low	15~150 m	9.6~40 kbps

The novelty of this research work is the implementation of a backoff algorithm with ADR to optimize the throughput, reduces the end-to-end delay for avoiding retransmission and overlapping of data packets, and minimizing the interference and congestion to make a reliable LoRa Network for ESL. The size of the contention window depends on the rate of the collision while the values of SF and DR depend on the allocation of the EDs from the gateway. Other works on the robustness of LoRa devices are done, avoiding the challenging characteristics of duty cycle, acknowledgment, and interference. In this research work, we use the LoRa network for our experiments to fully observe the difficulties associated with LoRa's long-range and test how various algorithms will perform with these challenges. Much research has already been done on designing the LoRaWAN network that is not capable to make a reliable network. LoRaWAN has several drawbacks. It cannot be used for large data payloads and is limited to 100 bytes, not for continuous monitoring (except Class C devices), not ideal candidates for real-time applications requiring lower latency and bounded jitter [5]. Moreover, the ESL designed before had certain limitations that include short-range and more energy consumption, while LoRa could not have the same weaknesses. The basic problems in LoRa are; using different gateways to transmit the same data, collision, data jamming, and data repeating are expected. According to the transmission behavior of LoRa, 50% of data is lost. Duty-cycle is only 1% of the total time during which the channel can be occupied [8]. This parameter arises from the ISM regulation as the key limiting factor for traffic served in the LoRaWAN network, the data packet having longer transmission time than duty-cycle is lost. The ALOHA mechanism can cause inefficiency by not eliminating fast saturation even with the increasing number of gateways [9]. The increasing number of gateways can only improve the global performance for generating packets with Poisson law having a uniform distribution of payload 1~51 bytes. To overcome these problems, some algorithms are used in this work to make an efficient LoRaWAN network. In order, to test the performance of our algorithm on a LoRaWAN, our experiment needs a simulation environment to examine all the relevant characteristics. By taking inspiration from various techniques for our algorithms, we have been able to observe the advantages and disadvantages of these different methods.

2 ESL Overview

The concept of ESL began in 1991 when Scandinavian tech-company Pricer was founded in Sweden. Pricer was the first one to install the ESL system in a Cash & Carry store in 1995. The ESL market has been expected to witness growth throughout 2024 when the global ESL industry is forecast to register more than 16% Compound Annual Growth Rate (CAGR). According to Maximize Market Research Company, the ESL market has a share of 350.5 million USD, which is expected to increase by 3088.51 million USD at CAGR of 24.31%. A study led by Allied Business Intelligence Research said that the global ESL market could reach 2000 million USD by 2019. At the moment, the market is grabbed by two types of commodity price display tools, the traditional price tag, and electronic shelf label. The traditional price tag is based on paper which is still used at the community supermarkets, and utility stores. This traditional price display system is controlled manually, and the paper price tag is changed after each variation in the price of the product. The update efficiency of this method is low, needs more manpower and time. The update speed is slow that causes customers' dissatisfaction. Moreover, this process involves the use of paper on a large scale which is not friendly for the environment. Printing, and material cost are also a big deal. To eliminate these issues, Electronic shelf labels were introduced. Electronic shelf labels have the capabilities of fast price adjustment to update the electronic price tag display for consumer satisfaction. This method is accurate, reliable, flexible, and easy to monitor. The background database, cash register, and price inquiry display are synchronized. Thus the involvement of manpower and paper is reduced. The current ESL is based on different network technologies that include NFC, Zigbee, RFID, BLE, etc. Kaufland Group, Altierre, Zkong, Pricer, Hanshow, MarillaTM Labels, DIGI, SES imagotag, and Rainus use NFC (needs more manpower). SoluM uses Zigbee (short-range), and M2COMM uses Wi-Fi (medium power consumption), Bluetooth (medium power consumption and short-range), BLE (short-range), and Zigbee while Ubiik uses UHF RFID readers (short-range with lack of standardization) [1,4,6,10,11]. To minimize these discrepancies, LoRa based ESL has been proposed. ESL is mainly composed of three parts, including the server, gateway, and node price tag group [12]. The number of gateways can be increased or decreased according to the size of the supermarket, and the number of node price tags as shown in Fig. 1.
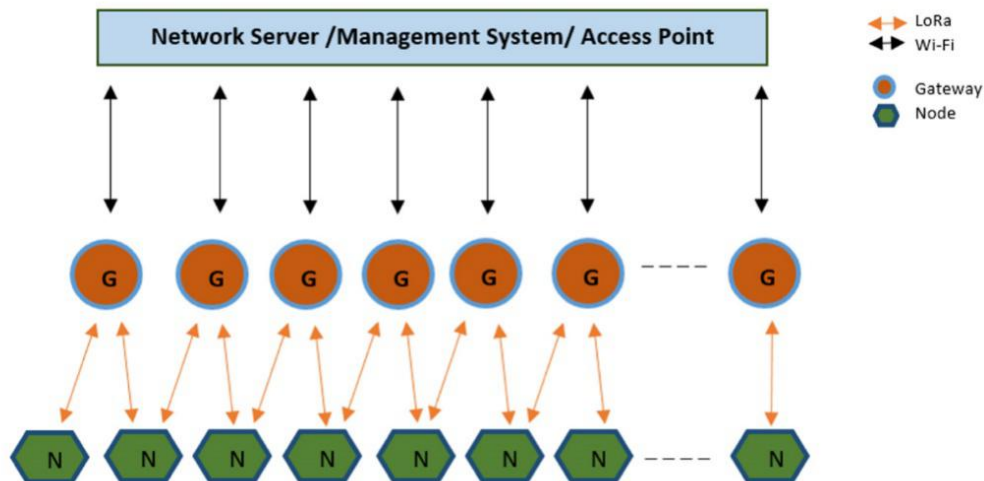
Figure 1: Sample of LoRa based ESL

While the system is running, the server is responsible for managing the entire system that includes changing the display of the node price tag and storing/managing the database of the entire supermarket goods. In changing the price tag, the first input data need to be changed by the server software. After computer analysis of transmitting data via serial port communication gateway, the gateway part is the main function of the system of data transmission, will come by the server to send data via LoRa communication transmitter to each node price tag. Gateway after receiving the data, the data is received

by the gateway analysis, and the data sorting, ordinal data transmitted LoRa communication way to each node. The node price tag is mainly used to display the price of supermarket goods. After receiving the data transmitted by the gateway, the LoRa module will analyze and process the received data to the e-paper module, and display it. The structure of the star topology network has been employed for the tagging system [13]. It seems stable, low power consumptive, and economical for maintaining quality communication among the gateways and scattered nodes. The network server is the center of star topology and has a great responsibility to optimize the data transmission rate and the transmission energy of the EDs, intending to optimize network scalability and energy intake with the help of ADR. The dynamical change in transmits power, frequency list, spreading factor, and uplink repeat rate are controlled by NS. The backoff algorithm improves the performance by adding a delay for collided or overlapped data packets that cannot be received successfully at the receiver side before. The delay depends on the history of the channel status. The performance of Improve ADR is considered by three main strategies, namely dynamic SF, different DR, and allocating least EDs to SF12 and SF7. Each LoRa device estimates the best SF configuration depending on the receiving power measured from the gateway.

3 Methodology

The methodology includes SF allocation and a DR model for Improved ADR to minimize the collision while backoff with synchronization is to avoid retransmission and data loss.

3.1 Improved ADR

ADR allows the NS to optimize the data transmission rate and the transmission energy of the EDs to intentionally optimize network scalability and energy intake [14]. The dynamical change in transmits power, frequency list, spreading factor, and uplink repeat rate happens [15]. This mechanism runs asynchronously, with low complexity in the end-devices and with more complexity within the network server. The ADR should only be enabled by using EDs in strong RF situations [16]. It aims to offer fairly reliable and battery-pleasant connectivity with the aid of adapting SF to changes in link conditions with the unique payload [17]. SF has a great impact, the higher value increases the sensitivity and range but long the airtime of a packet leads to the risk of collision. Each EDs and the network play an important function in this process. If a huge number of continuous uplink transmissions are observed by EDs that are not observed by a downlink response from the network, it assumes lost connectivity. To resolves this issue, gradually stepping up the SF and decreasing payload techniques are followed as shown in Fig. 2 [18–20].
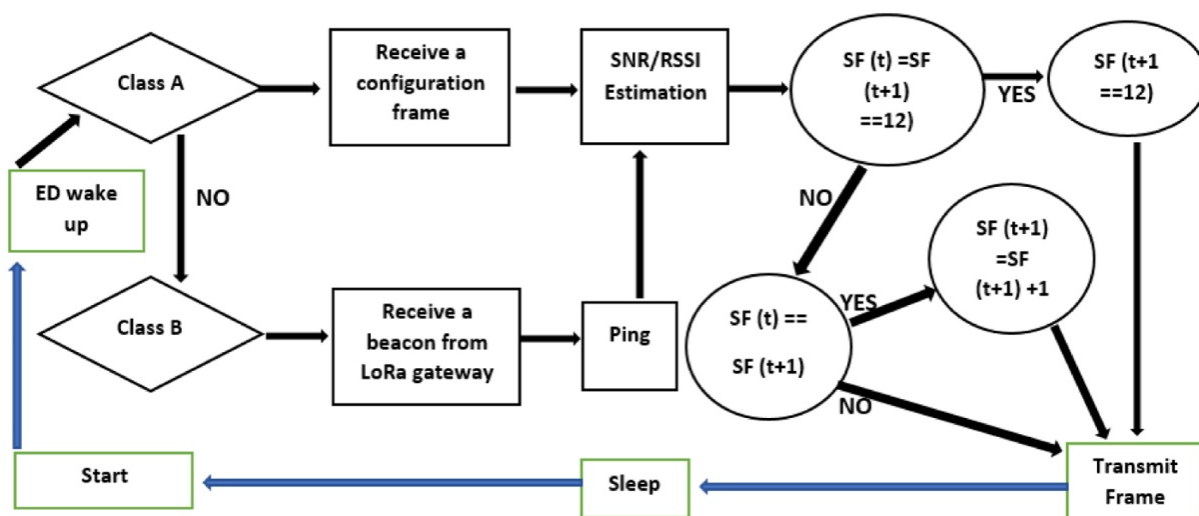
Figure 2: Flow chart of improved ADR

SF(t) illustrates the values of SF during transmission. Initially, SF(t) remains the same but steps up to SF(t+1) or SF(t+1)+1 depending on the condition of the channel and receptor. LoRa needs a lot of time to move from the lower to the higher SF(t) to regain connectivity because the process requires devices to lose a sufficient number of sent packets before moving to the higher SF(t). So, in improved ADR the SF(t) will directly jump to SF(t+1)+1 which acts like SF(t+1) to resume the connectivity with minimum packet loss.

3.1.1 SF Allocation

SF is the ratio between the symbol rate (RS) and the chip rate (RC), $SF = log_2(RS/RC)$ [21]. By changing SF each step from the lower value to higher, will take double airtime to transmit for the same data packet [22]. Thus, SF7 has the shortest airtime while SF12 has the longest airtime to travel a long distance. The value of SF is also depending on the range of transmission and status of the channel [23]. A good channel has a higher value of SF while the poor have a lower value. The value of CR (code rate) is 1, and BW (bandwidth) is 125 kHz to examine the importance of SF. The allocation of SF has the main role in designing LoRa based network to minimize the impact of intra-interference, cost function, and Euclidean distance. For this purpose, the *K*-means machine learning algorithm is used for clustering. It defines the more optimal solution to the clustering of large data sets. The centroid is chosen by the initial arbitrarily *K* point from the dataset. The other points are clustered to the closest centroid to recalculate its coordinates for cost function coverage. Initially, the number of centroids is chosen to determine the area of the annulus for the selection of SF. Each step of SF from 7 to 12, increases the annulus area that leads to the increment of node density due to uniform distribution. The inner (Ri) and outer ($Ri + 1$) radii of the annulus are well defined to choose the precise number of nodes for each value of SF as shown in Fig. 3.
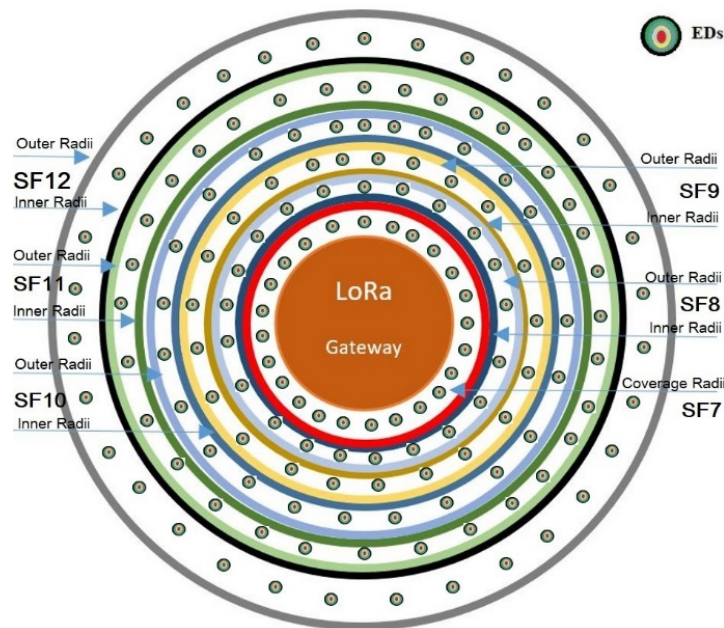
Figure 3: SF allocation

The method includes five steps of iterations to calculate the right number of nodes that start from the outer annulus of SF12 which acts as a network radius to the inner radii of SF8 [24–25].

$$C = \arg_{GW_k \in C} min \frac{1}{|ED_k|} \sum_{ED_i \in ED_k} dist(GW_k, ED_i)^2 \tag{1}$$

The number of connected EDs is directly proportional to the increasing step of SF due to variance in the area of each annulus. The network performance will affect if the difference between consecutive iterations is very big. A large number of EDs in that specific region would lead to a collision and co-SF interference, and for SF7 the coverage would be larger for more nodes if *K* is high in the last iteration.

EDs connected in the SF12 coverage area have more chances of collision for simultaneously transmitted data packets due to long airtime. To minimize the chances of collisions and co-SF interference, the K-means Spreading Factor algorithm is proposed. The remaining nodes are assigned to SF7. Tab. 2 shows the corresponding range, bit rate, receiver sensitivity, airtime, and SNR threshold for a payload of 16 bytes [24].

Table 2: SF v/s range, airtime, SNR, and receiver sensitivity

SF	Bit Rate (bps)	Sensitivity (dBm)	Range (km)	Airtime (ms)	SNR dB (qSF)
7	5468.75	−123	R_0-R_1 =0.7	59.65	−6
8	3125	−126	R_1-R_2=0.9	98.82	−9
9	1757.81	−129	R_2-R_3=1.1	177.15	−12
10	976.56	−132	R_3-R_4=1.5	354.3	−15
11	537.11	−134.5	R_4-R_5=1.6	626.69	−17.5
12	292.97	−137	2.1> R_5	1253.38	−20

3.1.2 Data Rate Model

The data rate model is using an intra-slicing technique based on MLE which includes three slices, HCC, MCC, and LCC as shown in Fig. 4 [26].
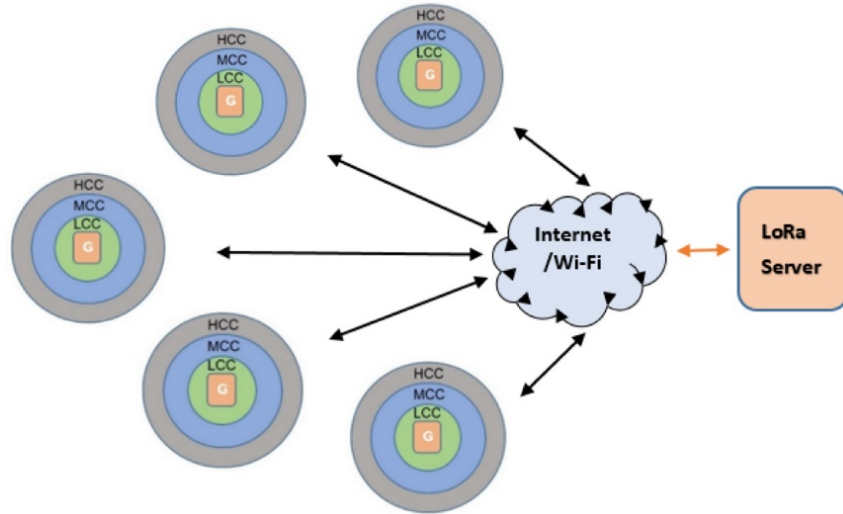
Figure 4: Data rate model

- HCC (High Critical Communication) requires the highest priority due to latency and collision. It will be used for those EDs that prices do not fluctuate daily.
- MCC (Medium Critical Communication) has less latency and collision than HCC. It is used for EDs that have normal fluctuation.
- LCC (Low Critical Communication) has the least latency and collision than HCC and MCC. It is used for high fluctuating EDs. Fig. 4 shows the design of the data rate model.

$$UHCC = \delta_r(w_r\sigma_r), \quad \delta_r \in \{0, 1\} \tag{2}$$

$$UMCC = \delta_r(w_r\sigma_r + w_{ld}\sigma_{ld}) \tag{3}$$

$$ULCC = \delta_r(w_{ld}\sigma_{ld}) \tag{4}$$

Every slice consists of w_r, w_{rld} reliability (multiple criteria weights), and load manipulation (analytical and hierarchy process approach), respectively. Each slice for the gateway offers the most robust and reliable link with the lowest delay, finds the highest UHCC metric, and allocates resources accordingly. Increasing the number of devices will decrease the reliability of links due to congestion. In

some cases, the most reliable link may be overloaded due to the increasing number of devices and should not be taken into consideration. Hence in Eq. (3), UMCC is defined to search for the flow that gives the best trade-off solution and offers the highest reliability with the lowest possible load. And finally, in Eq. (4), the ULCC slice includes delay-tolerant devices with high packet delay budgets. Therefore, only the load is considered in the latter without considering reliability.

3.2 Improved Backoff with Synchronization

This algorithm is especially proposed to improve the throughput and end-to-end delay which has a great impact on the performance of the network [27]. To achieve the desire performance, the adjustment of the increment/decrement procedure of the CW in the backoff algorithm is followed as shown in Fig. 5.
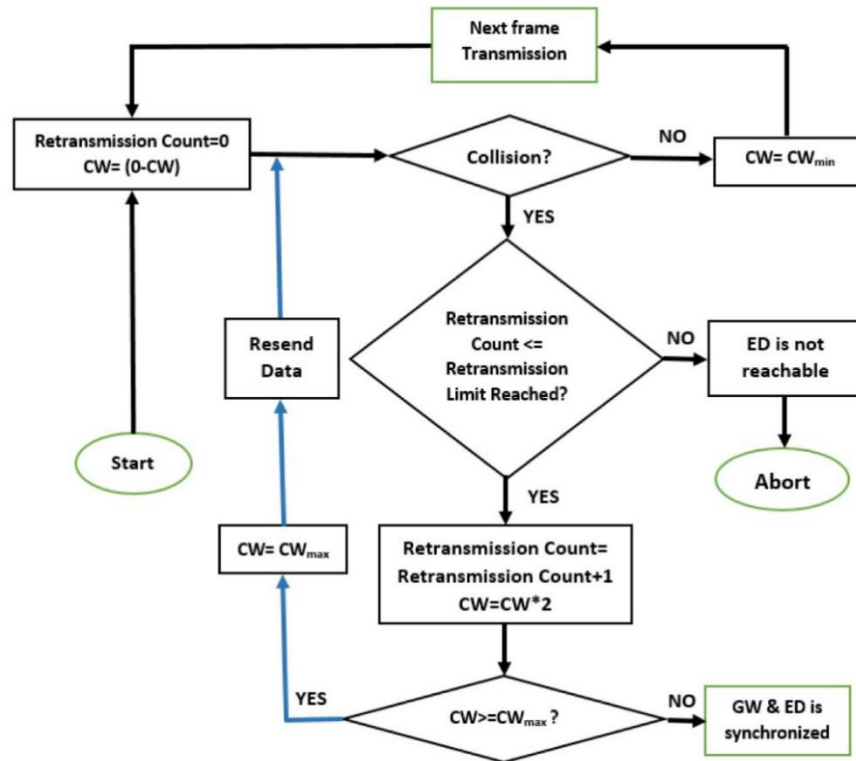
Figure 5: Flow chart of improved backoff algorithm with synchronization

In the basic Backoff algorithm, CW becomes doubled upon a collision until the frame is successfully transmitted or reaches the maximum number of retransmissions. CW is reset to CWmin after successful transmission which causes a decrement in throughput leads to termination of the transmission. In case of collision, CW can be mathematically represented as

$$\text{CWnext} = \text{CWprev} \times 2^{\alpha} \tag{5}$$

In general, α is static and equal to 1. For modification of the backoff algorithm, the best decision is always to ignore too short or too long backoff values. In the Improved Backoff Algorithm the value of α is diverse dynamically between -1 and 1, and is set by the equation, $\alpha = -1 + (2 * P)$. P represents the traffic load or collision rate, C means the number of collisions, and S means the number of successful transmissions while the variable β represents the order of collision or successful transmission and calculated by

$$P = \frac{C}{C+S} + \beta \tag{6}$$

$$P = \frac{C}{C+S} + abs(\beta) \tag{7}$$

$$\beta = \Sigma_{i=1}^{n-1} \left(\pm 10^{(i-n)} \times 5^{(n-i+1)} \times 10^{\left[\frac{n-i-1}{2}\right]} \right) \tag{8}$$

The $\pm$ sign is used to specify the transmission is a collision or successful, variable n represents the total number of transmissions. After the collision, the increment behavior for CW is changed by adding the absolute β to P which increases the waiting time for reducing the contention on the channel to increase the throughput of the network. For decrement of CW, β is ignored to avoid the channel capture effect. To improve the performance, the LoRa gateway (GW) is synchronized by continuously sending messages to the ED [8]. The ED will send ACK (acknowledgment) to the gateway about the reception of the message [18,23]. The ED is synchronized to the gateway's clock by subtracting the ToA (time on air) of the message from the message reception time. The gateway also performs the same by subtracting the ToA of ACK from the reception time of ACK. The backoff algorithm improves the performance by adding a delay for collided or overlapped data packets that cannot be received successfully at the receiver side before. Moreover, the gateway waits until ACK is received, and sends a new packet with counter time. If the packet is lost, the gateway will retransmit the previous packet in the backoff interval. If again does not receive the *ACK* for retransmission then the packet will be discarded, and the gateway will resend six symbols of the preamble to resynchronize the ED. If the data packet is pending in downlink communication, it means the gateway has more data pending to be sent. Thus by sending another uplink message to ask the ED to open another receive window as soon as possible.

4 Implementation and Result

This section includes configuration, condition, and performance evaluation.

4.1 Configuration and Condition for ADR

The performance of Dynamic ADR is evaluated with different SF configurations for a fixed number of 200 ED*s*. Three main strategies are considered, namely dynamic SF, different data rates, and allocating the least EDs to SF12 and SF7. Each LoRa device estimates the best SF configuration depending on the receiving power measured from the gateway. In configurations, the test is repeated for each SF value [17].

Table 3: Gateways and end devices

Parameter	Region	BW	SF	P_{TX}	NF	Side length	GW (D)
Value	EU868 MHz	125 kHz	7-12	14 dBm	6 dB	10000 m	5000 m
Parameter	Simulation(t)	Path loss		EDs	Gateways	L_{PL}(dB)	Packet/10m
Value	200 m	4.31		200	1,2,4,10	127.84	1

Table 4: Different combination of gateways

SF	12	11	10	9	8	7
R_SNR	−20	−17.5	−15	−12	-9	−6
M_SNR$_1$	−20.6885	−16.8336	−14.4322	−12.8473	−11.2519	−7.06654
Margin$_1$	−0.6885	0.6664	0.567843	−0.84730	−2.25193	−1.06654
M_SNR$_2$	−18.8479	−17.7323	−13.3864	−12.5934	−12.8398	−4.22396
Margin$_2$	1.15211	−0.2323	1.61358	−0.5933	−3.8398	2.27604
M_SNR$_4$	−19.614	−16.240	−15.2500	−9.92403	−7.64431	−8.24220
Margin$_4$	0.38599	1.25999	−0.2500	2.07597	1.35569	−2.2422
M_SNR$_{10}$	−23.7875	−16.9122	−13.8121	−9.99601	−8.8346	−4.09579
Margin$_{10}$	−3.7875	0.5878	1.18786	2.03990	0.16540	1.40421

However, for dynamic configurations, a gateway with a powerful receiving signal picks a small SF value whereas edge ED*s* are generally configured with larger SF values [18]. Packets may be lost when the ED is saturated due to the load in the network by co-channel rejection or lack of sensitivity when the packet is out of range of ED or when it does not reach the ED due to inappropriate SF configuration. To avoid these problems, more gateways are installed, and the distance of the gateway is kept in the range of SF12 EDs. When the transmissions of two LoRa gateways overlap at the EDs, several conditions

determine whether the ED can decode the frames or not [28]. These conditions depend on channel, SF, power, and timing. Tab. 3 displays the parameters.

4.1.1 Performance Evaluation

Positive values of Margin for demodulation represent strong signals while Negative values represent weak signals. LoRa has SNR below the noise floor (below zero), and the values of measured SNR (M_SNR) below the required SNR (R_SNR) are considered corrupt. Tab. 6 shows the comparison of R_SNR and M_SNR. The performance of the two gateways is better as compared to a single gateway, and more than half of the packets are delivered successfully. The packet sent at SF12, SF10, and SF7 are accepted by the receiver.

Table 5: Comparison of receiver sensitivity, link Budget, and receiver power of GWs

SF	12	11	10	9	8	7
R_Sensitivity(dBm)	−137	−134.5	−132	−129	−126	−123
R_LB (dB)	151	148.5	146	143	`140	137
R_P_{RX}	−123	−120.5	−118	−115	−112	−109
M_Sensitivity$_1$	−137.688	−133.8336	−131.4322	−129.8473	−128.2519	−124.0665
M_LB$_1$	151.6885	147.8336	145.4322	143.8473	142.2519	138.0665
M_P_{RX1}	−123.688	−119.8336	−117.4322	−115.8473	−114.2519	−110.0665
M_Sensitivity$_2$	−135.847	−134.7323	−13.3864	−129.5934	−129.8398	−121.2239
M_LB$_2$	149.8479	148.7323	144.3864	143.5934	143.8398	135.2239
M_P_{RX2}	−121.847	−120.7323	−116.3864	−115.5934	−115.8398	−112.2239
M_Sensitivity$_4$	−136.614	−133.240	−132.250	−126.924	−124.644	−125.242
M_LB$_4$	150.614	147.240	146.250	140.924	138.644	139.242
M_P_{RX4}	−122.614	−119.240	−118.250	−112.924	−110.644	−111.242
M_Sensitivity$_{10}$	−140.787	−133.912	−130.812	−126.996	−125.835	−121.096
M_LB$_4$	154.787	147.912	144.812	140.996	139.835	135.096
M_P_{RX10}	−126.787	−119.912	−116.812	−112.996	−111.835	−107.096

The four gateways perform better than the two gateways but still, the packets suffer at SF10 and SF7. On the receiver side, the sensitivity of the receiver is the value that affects the link budget. Tab. 5 represents the Comparison of Receiver Sensitivity (*Sensitivity $_{RX}$*) with Measured Sensitivity (M_Sensitivity), Link Budget (*LB*), and Receiver Power (*P_{RX}*). The *sensitivity $_{RX}$* describes the minimum possible reception power and tolerance for thermal noise and is calculated by the following formula:

$$Sensitivity_{RX} \text{ (dBm)} = -174 + 10 \, log_{10} \, (BW) + NF + SNR \tag{9}$$

Bandwidth in Hz, Noise factor in dB, and SNR. Transmission Power (P_{TX}) is 14 dBm, Bandwidth is 125 kHz = $10log_{10}$ (125000) = 51, and Noise Factor is 6 dB because gateways in LoRaWAN networks have lower values of NF. The Link budget indicates the quality of a radio communication channel.

$$LB \text{ (dB)} = P_{TX} \text{ (dBm)} - Sensitivity_{RX} \text{ (dBm)} \tag{10}$$

The Power received from each combination of gateways at the EDs is calculated by Eq. (11).

$$P_{RX} \text{ (dBm)} = P_{TX} \text{ (dBm)} + Sensitivity_{RX} \text{ (dBm)} \tag{11}$$

Fig. 6 shows the overall percentage of rejected packets for 200 EDs using a different number of gateways. This is the network performance of gateways without using the retransmission mechanism. Most of the packets of a single gateway are rejected which are decreased with the increasing number of gateways up to a certain limit. When ten gateways are implemented then only 17% of packets are rejected. The data rate and power consumption decrease when SF increases [23,29]. There are more chances of collision at higher SF while more chances of interference at lower SF [19]. The adaptive dynamic slicing

commercially adopted, slicing rate of every slice varies from a gateway to any other because MLE estimates the throughput of every slice contributor deployed in the range of the corresponding gateway.
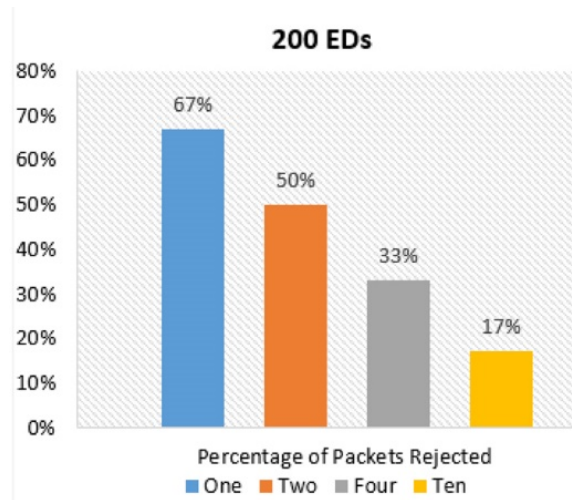
Figure 6: Packets rejection percentage
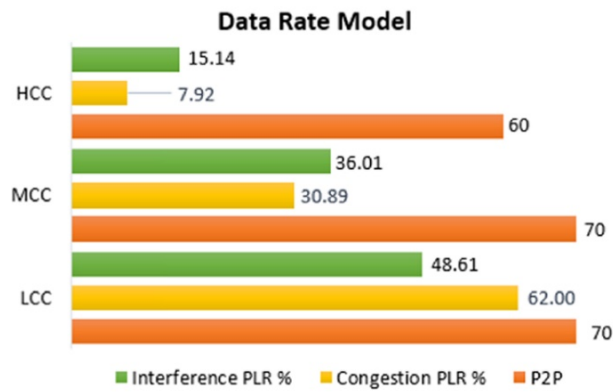
Figure 7: Data rate model based on slices

This configuration is the most reliable because SFs are dynamically configured on LoRa devices by measuring the receiving power that a gateway receives from the device relying on its position [30]. The benefits that the latter configuration present are depending on how far the device is from the gateway, a smaller distance requires a smaller SF configuration and the fact of adopting exclusive SF*s* configuration reduces interference (packet loss rate) PLR and the opportunity of collisions. Irrespective of the adopted SF configuration technique, the urgency character of HCC explains the low percentage in terms of PLR as compared to MCC and LCC slices. Urgent packets are not dispatched as often as other slices which reduces the possibility of packet collision. Fig. 7 displays the optimized performance of each slice for a bandwidth of 125 kHz, using a long-distance propagation model.

L(fs) is the free space losses in dB, D is the distance between the gateway and ED in kilometer while *f* is the frequency (868 MHz). Finally, the performance of ten gateways based on SF allocation and the DR Slicing Model are examined in the range of 0.7~2.1 km. The performance of the LoRa network has improved, and almost all the packets are delivered successfully without any ADR requests. The M_SNR is greater than the R_SNR.

$$L(fs) = 32.45 + 20\log(D) + 20\log(f) \tag{12}$$

Receiver Sensitivity, Link Budget, and Received Power are calculated based on Measured SNR. Tab. 6 shows that the signal is weaker at SF9 as compared to other SF*s*, and has a higher loss at SF12.

Table 6: Performance of ten gateways based on SF allocation and DR model

SF	Slice Model	R_SNR	M_SNR	Margin	Range (km)	L(fs) in dB
12	HCC (DR0)	−20	−18.1436	1.85637	2.1	97.664
11	HCC (DR1)	−17.5	−14.8198	2.68015	1.7	95.829
10	MCC (DR2)	−15	−11.8487	3.15133	1.6	95.302
9	MCC (DR3)	−12	−11.0484	0.95164	1.5	94.742
8	LCC (DR4)	−9	−7.36521	1.63479	1.1	92.048
7	LCC (DR5)	−6	−4.39303	1.70697	0.7	88.122
SF	7	8	9	10	11	12
Sensitivity(dBm)	−121.39303	−124.36521	−128.0484	−128.8487	−131.8198	−135.1436
Link Budget(dB)	135.39303	138.36521	142.0484	142.8487	145.8198	149.1436
RX Power(dBm)	−107.39303	−110.36521	−114.0484	−114.8487	−117.8198	−121.1436

4.2 Configuration and Condition for Backoff

The improved backoff algorithm is based on three variables; CW, *multiplicative factor* (2^α) for updating the CW and *Channel state*, and *Channel state* for representing the busy/free state. For unsuccessful transmission, the size of CW becomes double. *Channel state* defines the most recent history of the medium, Free State represents that none of the gateways is transmitting and the channel is available at the moment.

Table 7: CW updates

Current state	State	CW value
0(busy)	00(busy, busy)	CW = CW × 2^α
	01(busy, free)	CW = CW × 2^α
	10(free, busy)	CW = CW × 2^α
	11(free, free)	CW = CW × 2^α
1(free)	11(free, free)	CW = CW
	01(busy, free)	CW = CW
	10(free, busy)	CW = CW
	00(busy, busy)	CW = CW / 2^α

Table 8: Parameters

Parameters	Value
Radius	1000m
Number of EDs	200
Number of Gateways	10
Packet size	50 byte
Data Rate	DR5~DR0
SF	7~12
Path Loss Exponent	4.31
BW	125 kHz
Region	EU868 MHz

Tab. 7 illustrates that the busy channel is denoted by 0 while available by 1. When one of the gateways is transmitting then N = 2. So, the channel state is 01 which means that the medium had been busy then free [27,31]. After unsuccessful transmission, the value of CW is multiplied by 2^α and the gateway waits to transmit again by using the number of time slots according to the new value of CW. For two consecutive busy states, the new value of CW will be divided by 2^α. For simulation, the parameters are given in Tab. 8.

Table 9: Allocation of EDs, data rate, and packet delay budget.

SF	Data Rate	Packet Delay Budget (ms)	Number of EDs
12	DR0	300	20
11	DR1	300	30
10	DR2	200	40
9	DR3	200	40
8	DR4	100	40
7	DR5	100	30

Using SF allocation that is based on the *K*-means machine learning algorithm, and the DR model that is using an intra-slicing technique based on MLE is used. To evaluate the performance of improving the backoff algorithm, the simulation is divided into sections. CW is a minimum for the first transmission and a maximum for the retransmission. Tab. 9 shows the allocation of EDs, DR, and Packet Delay Budget for our work. $CW = CW \times 2^{\alpha}$

4.2.1 Performance Evaluation

When $CWnew = MAX [CWmin+1, CWprev \times 2^{\alpha}]$, $(\beta = 0)$, the following results are obtained.

Table 10: Analysis of improved backoff algorithm for CW_{new} (CW_{min})

SF	Packets	Delivered	Lost	α	2^{α}	CW_{min}	CW_{next}	CW_{new}	P
12	20	13	7	−0.30	0.8122	0.3	0.24366	1.3, 0.24366	0.350
11	30	23	7	−0.53	0.6925	0.3	0.20775	1.3, 0.20775	0.233
10	40	29	11	−0.45	0.7320	0.2	0.14640	1.2, 0.14640	0.275
9	40	35	5	−0.75	0.5946	0.2	0.11892	1.2, 1.11892	0.125
8	40	33	7	−0.65	0.6372	0.1	0.06372	1.1, 0.06372	0.175
7	30	26	4	−0.73	0.6029	0.1	0.06029	1.1, 0.06029	0.133

When $CWnew = MAX [CWmax + 1, CWprev \times 2^{\alpha}]$ and $(\beta = 1.58)$, the results obtained from the first retransmission for each value of SF are given below in Tab. 11.

Table 11: Analysis of improved backoff algorithm for CW_{new} (CW_{max})

SF	Packets	Delivered	Lost	α	2^{α}	CW_{max}	CW_{next}	CW_{new}	P
12	20	16	4	−0.60	0.6575	0.6	0.16020	1.6, 0.16020	0.20
11	30	26	4	−0.73	0.6029	0.6	0.11253	1.6, 0.11253	0.13
10	40	35	5	−0.75	0.5946	0.4	0.11892	1.4, 0.11892	0.14
9	40	38	2	−0.90	0.5335	0.4	0.08705	1.4, 0.08705	0.05
8	40	38	2	−0.90	0.5335	0.2	0.03399	1.2, 0.03399	0.05
7	30	28	2	−0.86	0.5509	0.2	0.03321	1.2, 0.03321	0.06

The performance of the LoRa network is improved in each slice, and the allocation of EDs will help to understand the behavior of the network. The technique will help in equal distribution of power and also minimize the far-near effect. The channel capture effect has become less due to ignoring β in the calculation of CW_{min}. The contention window has been minimized by β, enlarging the waiting time on the channel. Thus end-to-end delay has been reduced. The packets lost due to collision, interference, and overlapping are reduced up to a certain limit. The comparison in the performance of each slice based on the *K*-means machine learning algorithm is given in Fig. 8.

The performance of the LoRa network is improved in each slice, and the allocation of EDs will help to understand the behavior of the network. The technique will help in equal distribution of power and also

minimize the far-near effect. The channel capture effect has become less due to ignoring β in the calculation of CW_{min}. The contention window has been minimized by β, enlarging the waiting time on the channel. Thus end-to-end delay has been reduced. The packets lost due to collision, interference, and overlapping are reduced up to a certain limit. The comparison in the performance of each slice based on the K-means machine learning algorithm is given in Fig. 8.

Figure 8: Performance of improved backoff algorithm

5 Conclusion and Future Work

The different combinations of gateways display the variation in packet rejection rate. The performance of the network improves with an increasing number of gateways. HCC has minimum interference (15.14%) and congestion (7.92%) PLR while LCC has maximum interference (48.61%) and congestion PLR (62%) and MCC remain between LCC and HCC with 36.01% interference and 30.89% congestion PLR. The overall performance of ten gateways is 67% which means that 33% of the data packets are lost due to interference and congestion. By increasing the number of gateways further does not increase the performance of the network. Thus the combination of SF allocation and the DR model has enhanced the performance of the network to 100% with weaker signal reception at SF9 and higher losses at SF12 for 200 EDs. The improved backoff algorithm changes the CW according to the collision rate. Thus decreases end-to-end delay. The size of the CW is dynamic that utilizes the bandwidth to improve the throughput of the network. CW depends on the number of packets rejected, SF, and distance of the ED from the gateway. The change in the size of the CW for each SF has varied the ToA which has improved the throughput of each slice with minimum delay. The allocation of EDs helped to determine the existence of ED in the range of the LoRa network to avoid retransmission. Hence HCC has maximum and LCC has minimum throughput which means that at SF12 and SF11 the receptor has a long time to accept the data packet. Thus backoff mechanism has optimized the throughput to a certain level by minimizing the far-near effect. This work is based on simulation and needs to be examined in the real world to check the performance of the network. Our future work is the implementation of these simulation works in practical life and checks the performance of the network to make ESL based on LoRa that could be easily and cheaply available in the market for the consumers. Besides, the number of EDs would be increased to provide a vast range of ESL connectivity with fewer LoRa gateways.

Conflicts of Interest: The authors declare that they have no conflicts of interest to report regarding the present study.

References

[1]   J. Xu and W. Li, "Design of electronic shelf label based on electronic paper display," in *IEEE 3rd Int. Conf. on Consumer Electronics, Communications and Networks*, pp. 250–253, 2013.

[2]   H. Hong, Y. Ren, R. Tian and L. Xiao, "Electronic shelf label system based on public illuminating network," *IEEE Asia Pacific Conference on Circuits and Systems,* pp. 1103–1106, 2008.

[3]   Y. Wang and Y. Hu, "Design of electronic shelf label systems based on ZigBee," *IEEE 4th International Conference on Software Engineering and Service Science*, pp. 415–418, 2013.

[4]   T. M. Fernández-Caramés and P. Fraga-Lamas, "A review on human-centered IoT-connected smart labels for the industry 4.0," *IEEE Access*, vol. 6, pp. 25939–25957, 2018.

[5]   A. Augustin, J. Yi and T. Clausen, "A study of LoRa: Long range & low power networks for the internet of things," *Sensors*, vol. 16, no. 9, pp. 1466, 2016.

[6]   J. S. Lee, Y. W. Su and C. C. Shen, "A comparative study of wireless protocols: Bluetooth, UWB, ZigBee, and Wi-Fi," in *IECON 33rd Annual Conf. of the IEEE Industrial Society*, pp. 46–51, 2007.

[7]   T. Polonelli, D. Brunelli, A. Marzocchi and L. Benini, "Slotted aloha on lorawan-design, analysis, and deployment," *Sensors*, vol. 19, no. 4, pp. 838, 2019.

[8]   D. Zorbas, K. Q. Abdelfadeel, V. Cionca, D. Pesch and B. O. Flynn, "Offline scheduling algorithms for time-slotted lora-based bulk data transmission," in *IEEE 5th World Forum on Internet of Things,* pp. 949–954, 2019.

[9]   J. Haxhibeqiri, F. V. D. Abeele, I. Moerman and J. Hoebeke, "LoRa scalability: A simulation model based on interference measurements," *Sensors*, vol. 17, no. 6, pp. 1193, 2017.

[10] J. Ock, H. Kim, H. S. Kim, J. Paek and S. Bahk, "Low-power wireless with denseness: The case of an electronic shelf labeling system—Design and experience," IEEE Access, vol. 7, pp. 163887–163897, 2019.

[11] C. Perera, P. P. Jayaraman, A. Zaslavsky, D. Georgakopoulos and P. Christen, "Sensor discovery and configuration framework for the internet of things paradigm," in *IEEE World Forum on Internet of Things*, pp. 94–99, 2014.

[12] Y. P. Ma and W. R. Ma, "Design of electronic shelf tag system based on simpliciti," *International Journal of Engineering and Applied Sciences,* vol. 4, no. 9, pp. 59-62, 2017.

[13] B. Pan, X. F. Lian, M. A. A. Khan and T. Li, "Design and implementation of electronic shelf label system based on LoRa," *Telecommunication Engineering,* vol. 1, pp. 1–7, 2019.

[14] E. Sallum, N. Pereira, M. Alves and M. Santos, "Improving Quality-of-Service in LoRa Low-Power Wide-Area networks through optimized radio resource management," *Sensor and Actuator Network*, vol. 9, no. 1, pp. 10, 2020.

[15] M. Capuzzo, D. Magrin and A. Zanella, "Confirmed traffic in LoRaWAN: Pitfalls and countermeasures," in *IEEE 17th Annual Mediterranean Ad Hoc Networking Workshop*, pp. 1–7, 2018.

[16] D. Magrin, M. Capuzzo and A. Zanella, "A thorough study of LoRaWAN performance under different parameter settings," *IEEE Internet of Things Journal*, vol. 7, no. 1, pp. 116–127, 2019.

[17] S. Li, U. Raza and A. Khan, "How agile is the adaptive data rate mechanism of LoRaWAN?" in *IEEE Global Communications Conf.,* pp. 206–212, 2018.

[18] H. Mroue, B. Parrein, S. Hamrioui, P. Bakowski, A. Nasser *et al.,* "LoRa+: An extension of LoRaWAN protocol to reduce infrastructure costs by improving the Quality of Service," *Internet of Things*, vol. 9, pp. 100176, 2020.

[19] M. Bor and U. Roedig, "LoRa transmission parameter selection," in *IEEE 13th Int. Conf. on Distributed Computing in Sensor Systems*, pp. 27–34, 2017.

[20] M. C. Bor, U. Roedig, T. Voigt and J. M. Alonso, "Do LoRa low-power wide-area networks scale?," in *19th ACM Int. Conf. on Modeling, Analysis and Simulation of Wireless and Mobile Systems*, pp. 59–67, 2016.

[21] A. Rahmadhani and F. Kuipers, "When lorawan frames collide," in *12th Int. Workshop on Wireless Network Testbeds, Experimental Evaluation & Characterization*, pp. 89–97, 2018.

[22] A. Lavric, V. J. W. C. Popa and M. Computing, "Performance evaluation of LoRaWAN communication scalability in large-scale wireless sensor networks," *Wireless Communications and Mobile Computing*, pp. 1–9, 2018.

[23] D. Magrin, M. Capuzzo, A. Zanella and M. Zorzi, "A complete LoRaWAN model for single-gateway scenarios," arXiv preprint arXiv: 1912.01285, 2019.

[24] M. A. Ullah, J. Iqbal, A. Hoeller, R. D. Souza and H. Alves, "K-means spreading factor allocation for large-scale LoRa networks," *Sensors*, vol. 19, no. 21, pp. 4723, 2019.

[25] G. Zhu, C. H. Liao and T. Sakdejayont, "Improving the capacity of a mesh LoRa network by spreading-factor-based network clustering," *IEEE Access*, vol. 7, pp. 21584–21596, 2019.

[26] S. Dawaliby, A. Bradai and Y. Pousset, "Adaptive dynamic network slicing in LoRa networks," *Future Generation Computer Systems*, vol. 98, pp. 697–707, 2019.

[27] S. Manaseer and F. Badwan, "History-based backoff algorithms for mobile ad hoc networks," *Computer and Communications*, vol. 4, no. 11, pp. 37–46, 2016.

[28] R. Sanchez-Iborra, J. Sanchez-Gomez, J. Ballesta-Viñas, M. D. Cano and A. F. Skarmeta "Performance evaluation of LoRa considering scenario conditions," *Sensors*, vol. 18, no. 3, pp. 772, 2018.

[29] J. C. Liando, A. Gamage and A. W. Tengourtius, "Known and unknown facts of LoRa: Experiences from a large-scale measurement study," *ACM Transactions on Sensor Networks*, vol. 15, no. 2, pp. 1–35, 2019.

[30] S. Dawaliby, A. Bradai and Y. Pousset, "Network slicing optimization in large scale lora wide area networks," in *IEEE Conf. on Network Softwarization*, pp. 72–77, 2019.

[31] M. Albalt and Q. Nasir, "Adaptive backoff algorithm for IEEE 802.11 MAC protocol," *International Journal of Communications, Network and System Sciences*, vol. 2, no. 4, pp. 300, 2009.